Synthesis of Zinc Sulfide Clusters and Zinc Particles within Microphase-Separated Domains of Organometallic Block Copolymers

V. Sankaran, J. Yue, and R. E. Cohen*

Department of Chemical Engineering, Massachusetts Institute of Technology, Cambridge, Massachusetts 02139

R. R. Schrock and R. J. Silbey

Department of Chemistry, Massachusetts Institute of Technology, Cambridge, Massachusetts 02139

Received April 5, 1993. Revised Manuscript Received May 11, 1993

Block copolymers of methyltetracyclododecene (MTD) and bTAN(ZnPh)$_2$ [where bTAN = 2,3-*trans*-bis((*tert*-butylamido)methyl)norborn-5-ene] were prepared via ring-opening metathesis polymerization. Microphase-separated films of these copolymers exhibiting either lamellar or spherical morphology were reacted with hydrogen sulfide yielding zinc sulfide (ZnS) clusters within the organometallic domains. Clusters with diameters up to 30 Å were prepared and characterized by X-ray diffraction and electron microscopy. The effects of processing parameters such as temperature, copolymer morphology, and the presence of coordinating bases on cluster size were investigated, and the results were explained on basis of nucleation theory. Investigation of these clusters by X-ray photoelectron spectroscopy (XPS) revealed a distinct increase in their band-edge separation (5.7 eV for 30-Å clusters) relative to the bulk ZnS bandgap (3.5 eV) indicative of quantum size effects. Also investigated was the formation of zinc particles and clusters by thermal treatment of the block copolymer films.

Introduction

A major goal[1-5] in the field of cluster science is the synthesis of large quantities of monodisperse clusters. Another desirable but elusive goal has been a simple and reliable method to incorporate clusters in an organized fashion within suitable matrices to facilitate application and processibility. Attempts to achieve these objectives have led to cluster synthesis in colloidal suspensions,[6,7] vesicles,[8] reverse micelles,[9-12] sol-gels,[13] zeolites,[14] LB films,[15-17] microporous glass,[18] and polymers.[19-23]

We have been pursuing techniques of synthesizing semiconductor[24,25] and metallic clusters[26-28] within block copolymer films. Our technique takes advantage of the phenomenon of microphase separation commonly observed in block copolymers.[29-33] This phenomenon leads to the formation domains (diameter up to 50 nm) of narrow size distribution,[34] whose dimensions are determined by the block molecular weights. The form of the morphology depends on the block copolymer composition; to date, lamellar, cylindrical, spherical,[35] and ordered bicontinuous double diamond[36] morphologies have been identified.

(1) Anders, R. P.; Averback, R. S.; Brown, W. L.; Brus, L. E.; Goddard, W. A. I.; Kaldor, A.; Louie, S. G.; Moscovits, M.; Peercy, P. S.; Riley, S. J.; Siegel, R. W.; Spaepen, F.; Wang, Y. *J. Mater. Res.* **1989**, *4*, 704-736.
(2) Henglein, A. *Chem. Rev.* **1989**, *89*, 1861-1873.
(3) Steigerwald, M. L.; Brus, L. E. *Acc. Chem. Res.* **1990**, *23*, 183-188.
(4) Stucky, G. D. In Naval Research Reviews: Cluster Science; Office of Naval Research: Washington, DC, 1991, pp 45.
(5) Wang, Y.; Herron, N. *J. Phys. Chem.* **1991**, *95*, 525-532.
(6) Rossetti, R.; Ellison, J. L.; Gibson, J. M.; Brus, L. E. *J. Chem. Phys.* **1984**, *80*, 4464-4469.
(7) Herron, N.; Wang, Y.; Eckert, H. *J. Am. Chem. Soc.* **1990**, *112*, 1322-1326.
(8) Watzke, H. J.; Fendler, J. H. *J. Phys. Chem.* **1987**, *91*, 854-861.
(9) Lianos, P.; Thomas, J. K. *Chem. Phys. Lett.* **1986**, *125*, 299-302.
(10) Steigerwald, M. L.; Alivisatos, A. P.; Gibson, J. M.; Harris, T. D.; Kortan, R.; Muller, A. J.; Thayer, A. M.; Duncan, T. M.; Douglass, D. C.; Brus, L. E. *J. Am. Chem. Soc.* **1988**, *110*, 3046-3050.
(11) Kortan, A. R.; Hull, R.; Onila, R. J.; Bawendi, M. G.; Steigerwald, M. J.; Carroll, R. J.; Brus, L. E. *J. Am. Chem. Soc.* **1990**, *112*, 1328-1332.
(12) Pileni, M. P.; Motte, L.; Petit, C. *Chem. Mater.* **1992**, *4*, 338-345.
(13) Breitscheidel, B.; Zieder, J.; Schubert, U. *Chem. Mater.* **1991**, *3*, 559-566.
(14) Wang, Y.; Herron, N. *J. Phys. Chem.* **1987**, *91*, 257-260.
(15) Xiao, K. Z.; Baral, S.; Fendler, J. H. *J. Phys. Chem.* **1990**, *94*, 2043.
(16) Zhao, X. K.; Fendler, J. H. *Chem. Mater.* **1991**, *3*, 168-174.
(17) Zhao, X. K.; McCormick, L.; Fendler, J. H. *Chem. Mater.* **1991**, *3*, 922-935.
(18) Luong, J. C. *Supperlattices Microstruct.* **1988**, *4*, 385-390.
(19) Wang, Y.; Suna, A.; Mahler, W.; Kasowski, R. *J. Chem. Phys.* **1987**, *87*, 7315-7322.
(20) Andrews, M. P.; Galvin, M. E.; Heffner, S. A. *Mater. Res. Soc. Symp. Proc.* **1989**, *131*, 21-33.
(21) Möller, M.; Künstle, H.; Kunz, M. *Synth. Met.* **1991**, *41-43*, 1159-1162.
(22) Yuan, Y.; Fendler, J. H.; Cabasso, I. *Chem. Mater.* **1992**, *4*, 312-318.
(23) Ziolo, R. F.; Giannelis, E. P.; Weinstein, B. A.; O'Horo, M. P.; Ganguly, B. N.; Mehrotra, V.; Russell, M. W.; Huffman, D. R. *Science* **1992**, *257*, 219-223.
(24) Sankaran, V.; Cummins, C. C.; Schrock, R. R.; Cohen, R. E.; Silbey, R. J. *J. Am. Chem. Soc.* **1990**, *112*, 6858-6859.
(25) Cummins, C. C.; Schrock, R. R.; Cohen, R. E. *Chem. Mater.* **1992**, *3*, 1153.
(26) Ng Cheong Chan, Y.; Schrock, R. R.; Cohen, R. E. *Chem. Mater.* **1992**, *4*, 24-27.
(27) Ng Cheong Chan, Y.; Schrock, R. R.; Cohen, R. E. *J. Am. Chem. Soc.* **1992**, *114*, 7295-7296.
(28) Ng Cheong Chan, Y.; Craig, G. S. W.; Schrock, R. R.; Cohen, R. E. *Chem. Mater.* **1992**, *4*, 885-894.
(29) Meier, D. J. *J. Polym. Sci.: Part C* **1969**, *26*, 81-98.
(30) Sadron, C.; Gallot, B. *Makromol. Chem.* **1973**, *164*, 301-332.
(31) Noshay, A.; McGrath, J. E. *Block Copolymers: Overview and Critical Survey*; Academic Press: New York, 1977.
(32) Leibler, L. *Macromolecules* **1980**, *13*, 1602-1617.
(33) Bates, F. S.; Fedrickson, G. H. *Annu. Rev. Phys. Chem.* **1990**, *41*, 525.
(34) Hashimoto, T.; Tanaka, H.; Hasegawa, H. *Macromolecules* **1985**, *18*, 1864-1868.

0897-4756/93/2805-1133$04.00/0

Synthesis of a diblock copolymer with an organometallic block allows for the sequestering of metal atoms selectively into the domains,[37] within which clusters can in principle be grown in a controlled fashion. The details of our method and its relative merits in comparison with other techniques utilizing polymers have been discussed in previous papers.[24,25,27,28]

In a recent publication[38] we reported the synthesis of a polymerizable ligand bTAN [2,3-*trans*-bis{(*tert*-butylamido)methyl}norborn-5-ene] and its zinc derivative bTAN(ZnPh)$_2$. Also included was the preparation of diblock copolymers of bTAN(ZnPh)$_2$ with methyltetracyclododecene (MTD) using well-defined ring-opening metathesis polymerization (ROMP) initiator W(CH^{t}Bu)(NAr)(O^{t}Bu)$_2$ [Ar = 2,6-^{i}Pr$_2$C$_6$H$_3$]. Here we report the subsequent conversion of the zinc in the organometallic domains of the block copolymer films to either metallic clusters of zinc (Zn) or semiconductor clusters of zinc sulfide (ZnS) by appropriate thermal or chemical treatment. These clusters have been characterized by wide-angle X-ray diffraction (WAXS), transmission electron microscopy (TEM), and X-ray photoelectron spectroscopy (XPS). The size of the clusters formed depended on a number of processing parameters such as temperature, presence of surface active reagents, and morphology of the precursor polymer film; these observations are interpreted in terms of nucleation theory.[39]

Experimental Section

Chemicals and Reagents. Benzene was vacuum distilled from a flask containing calcium hydride (CaH_2) and stored over sodium–potassium (NaK) alloy. Prior to use benzene was filtered through a sintered-glass frit. MTD was vacuum distilled from sodium, stirred over Na/K alloy for 12 h, and filtered through a sintered-glass frit. Hydrogen sulfide (H_2S), C.P. grade, was purchased from Matheson. *trans*-1,3-Pentadiene was purchased from Aldrich, and stored over 4-Å molecular sieves prior to use. Bulk ZnS powder (99.99%, 10 μm size) was purchased from Aldrich. W(CH^{t}Bu)(NAr)(O^{t}Bu)$_2$ [Ar = 2,6-^{i}Pr$_2$C$_6$H$_3$] and bTAN(ZnPh)$_2$ were synthesized as described in literature.[38,40]

Polymer Synthesis. All polymerizations were performed at room temperature inside a Braun nitrogen glovebox using glassware flame dried under vacuum. Block copolymers of MTD and bTAN(ZnPh)$_2$ were synthesized by sequential addition of the monomers to W(CH^{t}Bu)(NAr)(O^{t}Bu)$_2$ in benzene, with the MTD block being polymerized first. The polymerization was terminated by the addition of a chain-transfer reagent, *trans*-1,3-pentadiene, which yields a vinyl-terminated polymer and a new tungsten alkylidene species. This new alkylidene is unreactive to our diblock.[38]

As an example, the procedure employed to prepare a 250/80 (values refer to numbers of repeat units) diblock of MTD/bTAN(ZnPh)$_2$ is described here. A solution of 3 mg (5.2×10^{-6} mol) of catalyst in 0.3 mL of benzene was added to a stirring solution of 227 mg (1.3×10^{-3} mol) of MTD in 3.7 mL of benzene. After 10 min, 2 mL of reaction mixture was withdrawn using a pipette and terminated with excess of benzaldehyde. This aliquot was used to obtain the molecular weight (via GPC) of the first block. A solution of 113.5 mg (2.1×10^{-4} mol) of bTAN(ZnPh)$_2$ in 4.0 mL of benzene was then added to the reaction mixture. After 30 min, 1.04 μL (1.1×10^{-5} mol) of pentadiene was added to terminate the polymerization. The reaction mixture was then stirred for another 1 h to ensure complete termination.

Films were solution cast directly from the polymerization mixture inside the nitrogen drybox. The polymerization mixture was transferred to a Teflon-lined glass cup and placed inside a sealed glass jar (diameter = 7 cm, height = 7 cm). The cap of the jar had a 1-mm-diameter hole. The solvent (benzene) was allowed to evaporate slowly over 5–8 days to obtain a transparent pale yellow film (the color is from the catalyst residue), which was further dried under vacuum for 24 h. The block copolymers formed rigid but readily handled glassy films; the polybTAN(ZnPh)$_2$ film was extremely brittle.

Formation of Metallic Zn Particles. Polymer films containing bTAN(ZnPh)$_2$ were sealed in a glass bomb reactor equipped with a Teflon stopcock inside the drybox. The bomb reactor was then taken out of the box, evacuated, and refilled with argon (UHP grade passed thru BASF oxygen scavenging catalyst and 4-Å molecular sieves). The reactor was then placed in an oil bath and heated to the desired temperature for 18 h. The sample was then cooled to room temperature and opened to air.

Hydrogen Sulfide Treatment. Polymer films containing bTAN(ZhPh)$_2$ were sealed in a glass bomb reactor equipped with a teflon stocpcock inside the drybox. The bomb reactor was then taken out of the box and evacuated using standard Schlenk tube techniques.

Room-Temperature Reaction. The evacuated bomb reactor was refilled with C.P. grade hydrogen sulfide (H_2S) and the reaction allowed to proceed for 18 h. The amount of H_2S gas added was controlled by setting the pressure gauge on the H_2S cylinder to 15 psig and opening the reactor to the cylinder for 10 s. At the end of the prescribed reaction time, the bomb reactor was opened to the atmosphere and the excess H_2S gas was allowed to dissipate over a period of 6–8 h. The sample was further pumped under vacuum to remove any residual H_2S.

High-Temperature Reaction. The evacuated bomb reactor was placed in an oil bath and heated to the desired temperature over ~2 h (if desired the reactor could be filled with argon prior to heating). The bomb reactor was then evacuated and refilled with H_2S in a manner identical to that for the room temperature reaction. The reaction was allowed to proceed for 18 h at 180 °C. The reactor was then cooled to room temperature and opened to air for 6–8 h to dissipate excess H_2S remaining in the reactor. Typically the sample was exposed to vacuum for an additional period of 3–4 h to remove any trace of H_2S.

Reaction in Presence of Solvents. Polymer films containing bTAN(ZnPh)$_2$ were sealed in a glass bomb reactor equipped with a Teflon stopcock inside the drybox. The sample was suspended above 0.5–1.0 mL of the selected solvent. The bomb reactor was then taken out of the box, partially evacuated and the sample allowed to soak in the solvent vapors for 12 h after which H_2S was introduced into the reactor. The H_2S reaction was then carried out in the presence of solvent vapors for a period of 18 h. Following this the reactor was opened to the atmosphere and the excess H_2S gas allowed to dissipate over 6–8 h. The sample was further pumped under vacuum at ~100 °C for 12 h.

Molecular Weight Characterization. Molecular weights were obtained by room-temperature gel permeation chromatography (GPC). The GPC setup comprised of four μ-Styragel columns (500, 10^2, 10^3, 10^4 Å) in series followed by a Knauer differential refractometer and a Spectroflow 757 absorbance detector (UV/vis detector). The solvent was tetrahydrofuran at a flow rate of 1.0 mL/min. The sample volume was 100 μL, and the concentration of polymer in the sample was ~0.2 wt %. The setup was calibrated using polystyrene standards (Polymer Laboratories Ltd.) ranging in molecular weight from 1.21×10^3 to 2.75×10^6 g/mol.

Morphology Characterization. All X-ray scattering experiments were performed on bulk samples using a Rigaku instrument with a 1.54-Å Cu Kα rotating-anode point source.

SAXS. The source was operated at 40 kV and 30 mA. The X-rays were focused with a Charles Supper double-mirror system and the scattered intensities collected on a Nicolet two-dimen-

(35) Helfand, E.; Wasserman, Z. R. In *Devleopments in Block Copolymers. 1*; Goodman, I., Ed.; Applied Science Publishers: London, 1982; Vol. 1, pp 99–126.
(36) Herman, D. S.; Kinning, D. J.; Thomas, E. L.; Fetters, L. J. *Macromolecules* **1987**, *20*, 2940–2942.
(37) Sankaran, V.; Cohen, R. E.; Cummins, C. C.; Schrock, R. R. *Macromolecules* **1991**, *24*, 6664–6669.
(38) Cummins, C. C.; Beachy, M. D.; Schrock, R. R.; Vale, M. G.; Sankaran, V.; Cohen, R. E. *Chem. Mater.* **1991**, *3*, 1153–1163.
(39) *Nucleation*; Zettlemoyer, A. C., Ed.; Marcel Dekker Inc.: New York, 1969.
(40) Schrock, R. R.; DuPue, R. T.; Feldman, J.; Yap, K. B.; Yang, D. C.; Davis, W. M.; Park, L.; DiMare, M.; Schofield, M.; Anhaus, J.; Walborsky, E.; Evitt, E.; Kruger, C.; Betz, P. *Organometallics* **1990**, *9*, 2262–2275.

sional detector. A helium-filled beam-line (2.4 m) was used to reduce atmospheric scattering. For each sample, the data were corrected for atmospheric scattering by subtracting a set of data obtained with no sample present.

WAXS. The source was operated at 50 kV and 60 mA and the Kβ radiation was eliminated by employing a Ni filter. The X-ray diffractometer and goniometer attachment were controlled by means of a MicroVAX computer running DMAXB Rigaku software. The slit system employed allowed for the collection of the diffracted beam with a divergence angle less than 0.2°. All diffraction data were collected in reflection mode with a step size of 0.05° and a collection time of 2.0 s/step.

TEM. Ultrathin sections (200–500 Å) obtained using a Sorvall MT-500 Ultramicrotome, were deposited onto copper grids. The microscopy was performed either on a Phillips EM-300 machine operating at 100 kV or a JEOL CX-200 machine operating at 200 kV. The high-resolution electron microscopy (HRTEM) was done on the Akashi EM-002B microscope operating at 200 kV. All samples were lightly carbon coated prior to HRTEM analysis. The precursor polymers were very difficult to section as they tended to hydrolyze during microtoming and disintegrate. However, the films were readily sectioned after treatment with H_2S.

X-ray Photoelectron Spectroscopy (XPS). XPS studies were conducted in a Perkin-Elmer photoelectron spectrometer with an aluminum Kα (1486.6 eV) source. In the case of insulating materials it is uncertain whether the necessary alignment of the Fermi level has taken place and whether an equilibrium condition is maintained in the sample-spectrometer system during the process of the measurement. This results in an X-ray-induced Fermi-level shift. In addition one observes charging effects arising from electron emission. Both of these were corrected for by referencing all core-level peaks to the carbon (C) 1s peak of the polymer matrix. We determined that the C 1s peak of the polymer matrix has the same full width at half-maximum (fwhm) as that of adventitious hydrocarbon on bulk ZnS powder; therefore the binding energy of the polymer C 1s peak was adjusted to 284.6 eV.[41]

The Zn 2p and 3d spectra, after background subtraction (two point), were decomposed into components consisting of a Gaussian line shape with a Lorentzian broadening function. Fitting parameters, including the widths and intensities, were freely adjustable and determined for each spectrum with an iterative least-squares fitting routine.[42]

Results

General Information Concerning the Monomer. The bTAN(ZnPh)$_2$ monomer was synthesized as described in the literature[38] as a white crystalline powder. Thermogravimetric analysis (TGA) of indicates that the monomer decomposes on heating, losing up to 60% of its weight by 210 °C (Figure 1). The degradation occurs in two distinct stages, with about 8.5% of the weight loss occurring in the first step (30–70 °C). The next step centered around 160 °C accounts for the bulk of the weight loss. Presumably the degradation involves destruction of the Zn–N bond and the Zn–phenyl bond, but the exact nature of the decomposition products has not been determined. The monomer also reacts cleanly with H_2S to yield the bTAN ligand and ZnS as the only products. This result was demonstrated by sealing 20 mg of bTAN(ZnPh)$_2$ monomer in a glass bomb reactor filled with H_2S and allowing it to react for 12 h at room temperature. Extraction of the reaction product by deuterated benzene and analysis by NMR indicated only the presence of the bTAN ligand.

(41) Wagner, C. D.; Riggs, W. M.; Davis, L. E.; Moulder, J. F.; Muilenberg, G. E. *Handbook of X-ray Photoelectron Spectroscopy*; Perkin-Elmer Corp.: Eden Prairie, MN, 1979.

(42) *Practical Surface Analysis: by Auger and X-ray Photoelectron Spectroscopy*; Briggs, D., Seah, M. P., Ed.; John Wiley & Sons: New York, 1983.

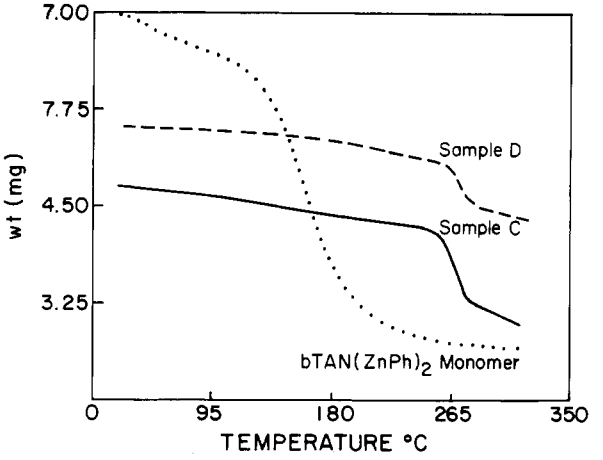

Figure 1. TGA data collected for the monomer, sample C and sample D from 30 to 300 °C.

Scheme I. Sequential Polymerization of MTD and bTAN(ZnPH$_2$) Using the W(CH^{t}Bu)(NAr)(O^{t}Bu)$_2$ Initiator [where Ar = 2,6-C$_6$H$_3$^{i}Pr$_2$]

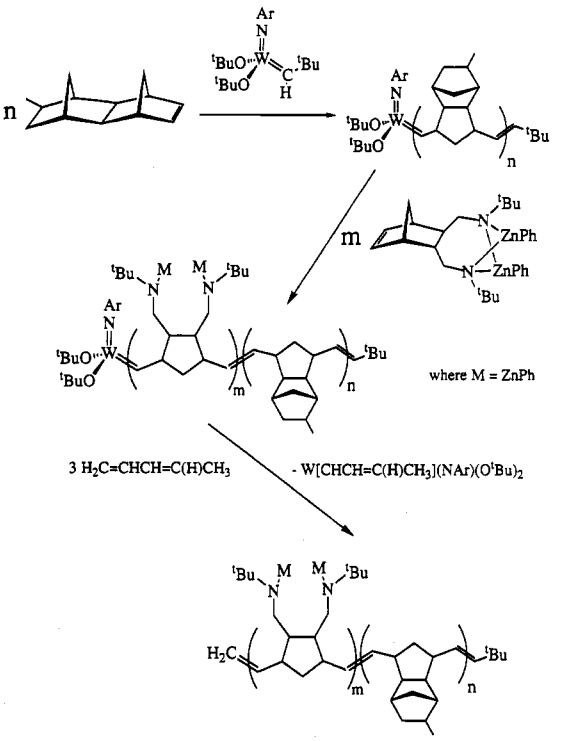

General Information Concerning Polymers. All polymers were synthesized with ring-opening metathesis polymerization (ROMP) initiators by sequential addition of monomers (Scheme I). Diblock copolymers of MTD and bTAN(ZnPh)$_2$ with specific ratio of block lengths were prepared to target either lamellar or spherical morphology. The composition and molecular weights for the various polymers synthesized are summarized in Table I. Molecular weights could only be determined directly for the first block because the bTAN(ZnPh)$_2$ block is extremely susceptible to hydrolysis and oxidation. Proof for the successful synthesis of diblocks comes from the low polydispersities of the first block, the compositions (proton NMR) of the final products and the ability to achieve the desired morphologies.[37,38]

TGA analysis of the homopolymers and diblocks indicated that the samples slowly lose a small fraction of their weight until a temperature of 240 °C (Figure 1). After 240 °C there is a significant weight loss with bulk of the loss

Table I. Summary of the Characterization of the Different Block Copolymers Synthesized

sample	diblock composition [MTD/bTAN-$(ZnPh)_2$], equiv	expected mol wt ($M_w \times 10^{-3}$) in [MTD/bTAN-$(ZnPh)_2$], g/mol	obsd[a] mol wt (M_w) of polyMTD block (PDI),[b] g/mol	wt fraction of bTAN $(ZnPh)_2$ block
A	250/80	43.6/43.9	79 000(1.06)	0.50
B	600/40	104.6/22.0	187 600(1.1)	0.17
C	0/200	0/109.9		1.00
D	250/80	43.6/43.9	55 768(1.05)	0.50

[a] Molecular weights as determined by GPC. Values reported are polystyrene-equivalent molecular weights. [b] PDI indicates polydispersity index, i.e., M_w/M_n.

Table II. Morphology and Interdomain Spacing (d') for the Different Samples

sample	wt fraction of bTAN $(ZnPh)_2$ block	morphology as determined by TEM	interdomain spacing (d') obtained using SAXS, Å	
			untreated[b]	treated[a]
A	0.50	lamellar[a]	410	420
B	0.17	spherical[b]	460	450
C	1.00			
D	0.50	lamellar[a]	490	485

[a] Determined using samples reacted at room temperature with H_2S. [b] Determined prior to H_2S treatment.

occurring around a temperature of 260 °C. Some part of the weight loss occurring at low temperatures could come from solvent trapped in the films during solution casting. These results indicate that the thermal stability of the polymers is greater than that of the monomer.

The morphologies obtained for the various diblocks as determined by TEM and SAXS are listed in Table II. As mentioned in the Experimental Section, the diblock copolymers were extremely difficult to section prior to H_2S treatment; the films tended to disintegrate during the microtoming process due to hydrolysis of the organometallic block. After considerable effort a reasonable section of sample B was obtained and found to exhibit a distorted spherical morphology (Figure 2). The zinc in the organometallic block acts as an inherent stain, resulting in the contrast observed in the micrographs; the dark regions correspond to the bTAN$(ZnPh)_2$ block. As expected the TEM data[43] indicate that copolymer A and copolymer D both with 50 wt % of the Zn block exhibit lamellar morphology (based on films reacted with H_2S at room temperature) while copolymer B with 17 wt % of the Zn block has the distorted spherical morphology. These observations are consistent with our previous observation for similar organometallic diblock copolymer systems.[37] The TEM results were qualitatively confirmed by our SAXS data. As shown in Figure 3, a typical two-dimensional SAXS spectrum is a clearly discernible ring at a particular value of the scattering vector Q. The scattering vector is related to the scattering angle 2θ by the expression $Q = (4\pi/\lambda) \sin \theta$, λ being the wavelength (1.54 Å) of the X-rays. The symmetry in the pattern is indicative of a macroscopically isotropic sample, with no preferred large-scale orientation of the morphology. This absence of long-range order is a consequence of our film preparation technique (solvent casting). The two-dimensional spectrum was converted to a plot of intensity (I) vs Q by taking an azimuthal average at each value of Q. The interdomain spacing ($d' = 2\pi/Q_{max}$) for each of the

(43) V. Sankaran, Ph.D. Thesis, MIT Department of Chemical Engineering, 1993.

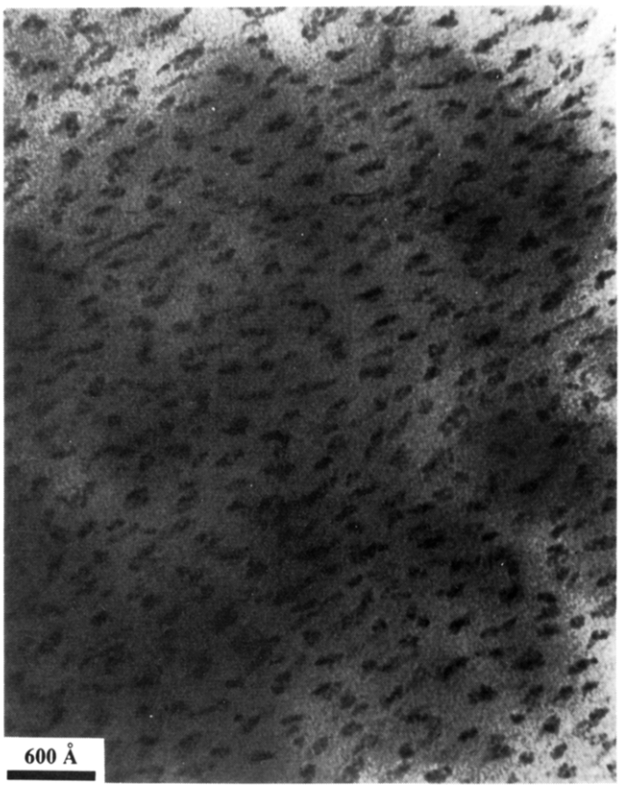

Figure 2. Typical TEM micrograph of sample B prior to reaction with H_2S.

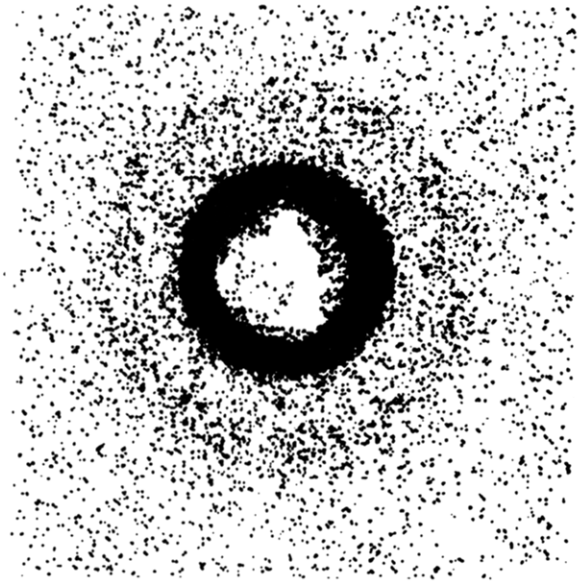

Figure 3. SAXS data obtained for sample A after background subtraction.

copolymers was obtained from the location of the maximum in the I vs Q plot. These morphological distances are listed in Table II. The values for d' obtained using SAXS are always higher than those obtained by TEM. This discrepancy has been observed previously and is discussed in one of our prior publications.[37]

Formation of Zinc Particles. Results for the TGA and DSC clearly indicate that the monomer decomposes on heating. Thermal treatment of the polymer films might therefore result in the formation of metallic zinc clusters within the organometallic domains. Films prepared from the various polymers listed in Table I were heated under an argon atmosphere at 240 °C in an attempt to synthesize Zn clusters. The results for samples A, C, and D were

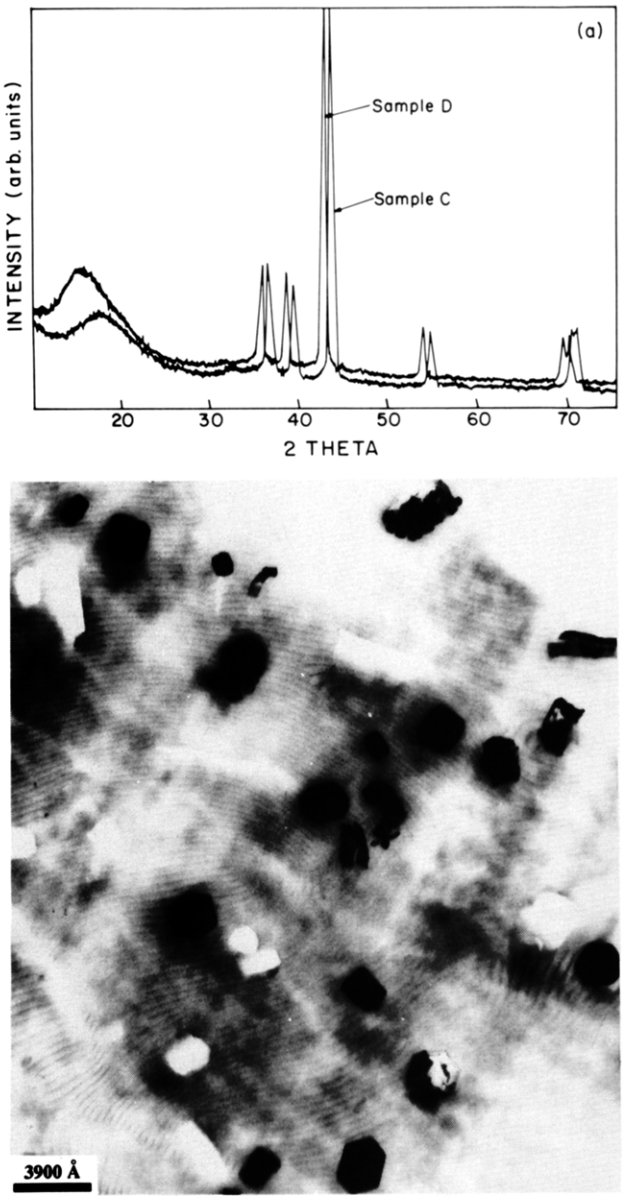

Figure 4. (a) X-ray diffraction (WAXS) spectra of sample C and sample D (shifted left ~10) after heating under an argon atmosphere at 240 °C for 18 h. Peak at $2\theta = 18°$ is from polyMTD. (b) Representative TEM micrograph for sample D after heating under an argon atmosphere for 18 h at 240 °C.

similar, but sample B (discontinuous spherical domains) behaved in a significantly different way. We shall therefore discuss the results obtained for sample B separately. X-ray diffraction (WAXS) analysis of the thermally treated films indicated the formation of large Zn particles in films of sample A, C, and D (Figure 4a). The WAXS spectra have six sharp peaks representing periodic spacings of 2.45, 2.28, 2.07, 1.68, and 1.34, and 1.32 Å and a broad peak indicating a spacing of about 5.4 Å. The broad peak can be attributed to the amorphous MTD block. The six sharp peaks correlate exactly with the expected spacings for bulk crystalline zinc in its hexagonal form.[44] These results were confirmed by TEM analysis of thin sections of the thermally treated polymer films, which indicate the presence of micron-sized particles (Figure 4b). The size of the zinc particles are therefore neither limited by the block copolymer domain size nor in any significant way restricted by the polymer matrix. The particle size

(44) *Selected Poweder Diffraction Data for Minerals*, 1st ed.; Berry, L. G., Ed.; JCPDS: Philadelphia, 1974.

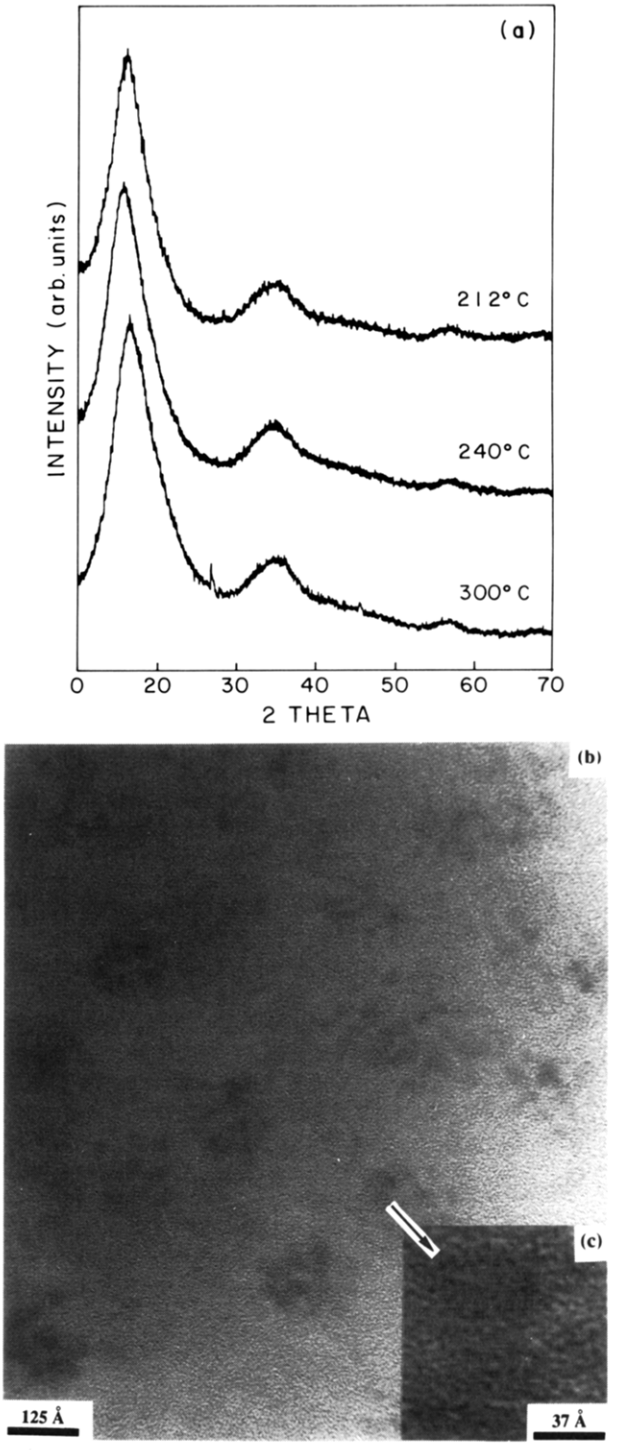

Figure 5. (a) X-ray diffraction (WAXS) data for sample B after heating under an argon atmosphere at various temperatures for 18 h. (b) TEM micrograph for sample B after thermal treatment at 300 °C in an argon atmosphere. (c) HRTEM micrograph of a large cluster showing lattice fringes.

distribution in fact suggests a nucleation/growth process accompanied by a Ostwald-like ripening (see the Discussion section for further details).

In the case of sample B thermal treatment at 212 or 240 °C did not result in the formation of large crystalline Zn particles as determined by X-ray diffraction (Figure 5a). The WAXS data in addition to the amorphous MTD peak show three very broad peaks centered at d = 2.60, 1.63, and 1.38 Å. This is not in any way related to the glassy nature of the MTD matrix because repeating the treatment at a higher temperature of 300 °C (T_g of MTD is ~210 °C[45]) yields similar results (Figure 5a). TEM analysis of

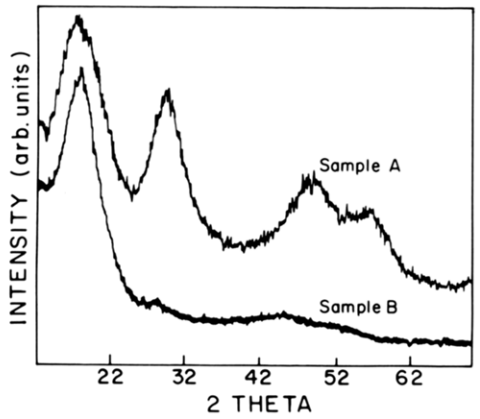

Figure 6. WAXS spectra collected for sample A and sample B after reaction with H_2S at room temperature.

the film treated at 300 °C reveals the presence of 7–15 clusters (roughly 20–25 Å in diameter) within each spherical domains (Figure 5b). High-resolution TEM did indicate the presence of lattice fringes in some of the clusters (larger ones), but most of the clusters are probably imperfect crystals. These crystal imperfections together with the size of these clusters would explain the broad X-ray diffraction peaks observed.[46]

Formation of ZnS Clusters. *Room-Temperature Synthesis.* Exposure of the block copolymer films containing bTAN$(ZnPh)_2$ to H_2S at room temperature resulted in the formation of zinc sulfide clusters as confirmed by X-ray diffraction. For these room-temperature preparations, there was essentially no difference in terms of cluster size between the block copolymer films exhibiting different morphologies. Representative WAXS spectra for films of samples A and B are presented in Figure 6. Each spectrum essentially exhibits three broad peaks at 2θ = 28.3°, 46.9°, and 55.6° which correspond to periodic lattice spacings (d) of 3.15, 1.90, and 1.66 Å. In addition to these three peaks, there is the peak at $2\theta \sim 16.0°$ which is the amorphous scattering from the MTD block. Bulk zinc sulfide can exist in either the cubic (d = 3.123, 1.912, and 1.633 Å) or the hexagonal (d = 3.309, 3.128, 2.925, 1.91, 1.764, and 1.63 Å) crystalline form.[44] The reasonably close match of either form to our diffraction pattern confirms the formation of crystalline ZnS within the polymer films. The broad peaks however make it difficult to assign a unique crystal structure. We can also infer from the broad peaks that these clusters are extremely small in size. Line-broadening analysis using Scherrer's formulas yields an average particle dimensions of ~20 Å for these clusters. However, it is important to note that Scherrer's formulas do not yield quantitatively accurate values for such small particles.

Electron micrographs of the room temperature treated films clearly indicate that the original block copolymer morphology is retained (Figure 7). This was also confirmed by SAXS which indicates that there is no change in the interdomain spacing after treatment with H_2S (Table II). Elemental analysis of the samples by X-ray fluorescence spectroscopy[47,48] (using a VG-HB5 STEM) shows that the Zn atoms are restricted to only one domain (the bTAN-

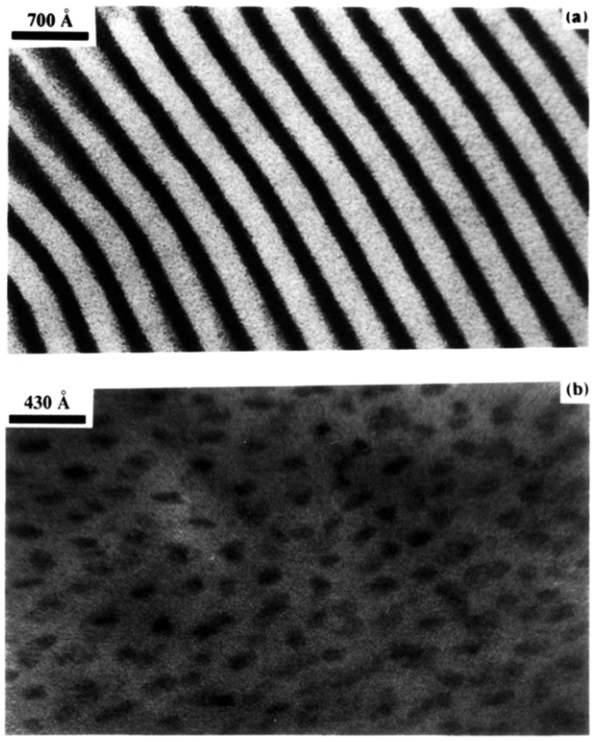

Figure 7. Typical TEM micrographs of sample A and sample B after room temperature reaction with H_2S: (a) sample A; (b) sample B.

Table III. Binding Energies[a] of Zn 2p and Zn 3d Core Levels from ZnS

core level	E_{bulk}	E_{sur}	E^{shift}	fwhm
bulk ZnS 2p	1021.5	1022.7	1.2	2.5
HT cluster 2p	1021.4	1022.4	1.0	2.4
RT cluster 2p		1023.3	1.8	1.9
bulk ZnS 3d	10.2	11.2	1.0	1.8
HT cluster 3d	10.3	11.2	0.9	1.7
RT cluster 3d		12.0	1.8	1.5

[a] All units are in electronvolts. E_{bulk} is binding energy for the bulk component, E_{sur} is binding energy for the surface component, and E^{shift} is $E_{sur} - E_{bulk}$.

$(ZnPh)_2$ domain) and the concentration of S atoms in the Zn-containing domains is considerably more than that in the matrix. In addition we were able to discern weak lattice fringes in the TEM within the Zn-containing domains; the fringes were too poorly formed to show up well in photographs taken.

All of these data in conjunction with the WAXS results support the contention that domain-confined ZnS clusters smaller than about 20 Å were formed in the room-temperature treated films. However we were unable to clearly discern any individual clusters in the TEM micrographs, probably due to overlapping of the 2-D projections of the clusters within each domain (typical thickness for a TEM sample was ≥100 Å). Additional evidence that the ZnS clusters formed are indeed very small comes from XPS analysis of these films which indicates a bandgap of 6.3 eV for the clusters. This is considerably larger than the bulk ZnS bandgap of 3.5 eV (see Table III and XPS characterization section for more details).

The small size of the ZnS clusters was not entirely unexpected. The H_2S treatment is done at a temperature considerably below the melting temperature of crystalline ZnS, and this could lead to extensive nucleation and hence numerous tiny clusters within each domain. On the basis of the observations of previous researchers we hoped to

(45) Schnider, W. U.S. Patent 4,320,239, 1982.
(46) Guinier, A. *X-Ray Diffraction: In Crystals, Imperfect Crystals and Amorphous Bodies*; W. H. Freeman and Co.: San Francisco, 1963.
(47) *Practicle Scanning Electron Microscopy*; Goldstein, J. I., Yakowitz, H., Ed.; Plenum Press: New York, 1975.
(48) Gebizlioglu, O. S.; Cohen, R. E.; Argon, A. S. *Makromol. Chem.* **1986**, *187*, 431–439.

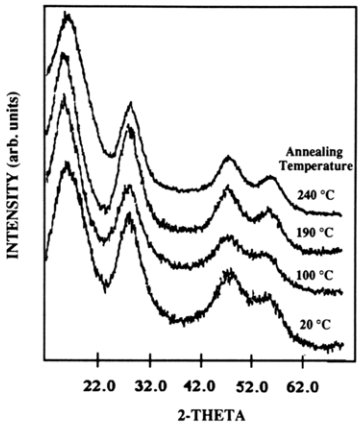

Figure 8. WAXS data for films of sample A annealed at various temperature after reaction with H_2S at room temperature.

Scheme II. Illustration of the Possible Polymer–Cluster Interaction Occurring via the Coordination of the Amine Groups in the Polymer to the Zn Atoms on the Surface of the Cluster

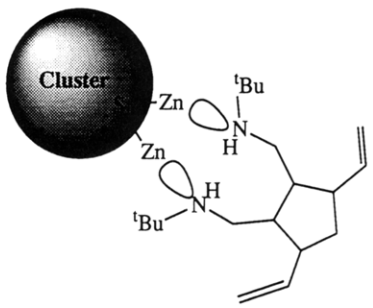

increase cluster size by annealing the polymer–cluster composites under suitable conditions.[19,21] We annealed our films incorporating ZnS clusters at 100, 190, or 240 °C under an argon atmosphere for 24 h. Analysis of the annealed films by WAXS gave results identical to those for the preannealed films (Figure 8), indicating no change in cluster dimensions. These results were also supported by TEM examinations of the different films. The tiny zinc sulfide clusters are therefore very stable, an extremely surprising finding. We believe that the stability of these tiny clusters arises from polymer–cluster interactions, the most likely being coordination of the amine groups of the polymer to zinc atoms on the surface of the cluster (Scheme II). The polymer therefore plays the same role as the capping agents used in the synthesis of semiconductor clusters via colloidal or reverse micellar techniques.[7,11,49]

High-Temperature Synthesis. Cluster formation is essentially a crystallization process with the polymer acting as the solvent and the size of cluster formed should depend on the kinetics of nucleation and growth. Increasing the temperature toward melting point should decreases nucleation; thus carrying out the H_2S reaction at a higher temperature should lead to the formation of larger clusters. This was found to be true for the copolymer films exhibiting both lamellar and spherical morphology. As seen in Figure 9, the WAXS pattern is much sharper for the high-temperature reaction than the room-temperature case (Figure 6) indicating an increase in cluster size. The TEM micrographs for sample A and B after reaction with H_2S at 180 °C are shown in Figure 10. The picture clearly shows dark, roughly spherical clusters within the organometallic domains. These clusters are approximately 30 Å in diameter, which correlated well with that obtained by line-broadening analysis of the WAXS data. Also shown in Figure 10c is a high-magnification view of a single spherical domain clearly showing seven or eight individual clusters.[50] The orientation of one of these clusters with respect to the electron-beam is such that the atom–column positions are visible. This particular cluster also shows a clearly discernible stacking fault.

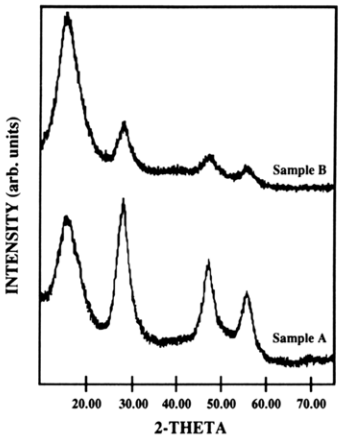

Figure 9. Diffraction (WAXS) spectra obtained for sample A and sample B after reaction with H_2S at high temperature.

We were unable to increase the cluster size further by carrying out the reaction at even higher temperatures due to decomposition of the bTAN$(ZnPh)_2$ polymer. As mentioned earlier, the Zn–polymer decomposes near 240 °C; repeating the high-temperature experiment at 240 °C results in the formation of micron-sized Zn particles coated on the outside with ZnS. Further investigation may enable controlled synthesis of well-defined core-shell structures of this type.

Solvent Effect on Cluster Synthesis. We were able to increase cluster size by carrying out the H_2S reaction at room temperature in the presence of certain solvent vapors. The procedure involved exposing the copolymer films to vapors of a desired solvent prior to reaction with H_2S. Figure 11 shows WAXS data for clusters prepared at room temperature in the presence of pyridine (Py) and dimethoxyethane (DME) together with those synthesized at room temperature (no solvent) and high temperature (180 °C). The clusters formed at room temperature with the solvent present are as large as those formed in the high-temperature experiment. We also tried benzene, tetrahydrofuran (THF), 2,6-lutidine, 4-picoline, triethylamine (Et_3N), dimethyl sulfoxide (DMSO), and triethylphosphine oxide. The best results were obtained for Py, with DME and 4-picoline also doing a reasonable job.

The cluster size (estimated from TEM and WAXS experiments) does not depend significantly on the compatibility of the solvent with the copolymer. For example, THF and benzene did not yield large clusters even though they are much better solvents than Py, DME, or 4-picoline for either polyMTD or polybTAN$(ZnPh)_2$. Cluster size also does not depend on the compatibility of the solvent with ZnS as neither Py, DME, or 4-picoline dissolve bulk ZnS (~10-μm size). Even more intriguing is the success of Py in comparison to 2,6-lutidine. Both these solvents dissolve polybTAN$(ZnPh)_2$ and swell polyMTD to the

(49) Steigerwald, M. L.; Brus, L. E. *Annu. Rev. Mater. Sci.* **1989**, *19*, 471–495.

(50) The spherical domains in sample B are roughly 150 Å in diameter and based on a Zn atom mass balance one would expect to form eight zinc sulfide clusters each with a diameter of ~30 Å.

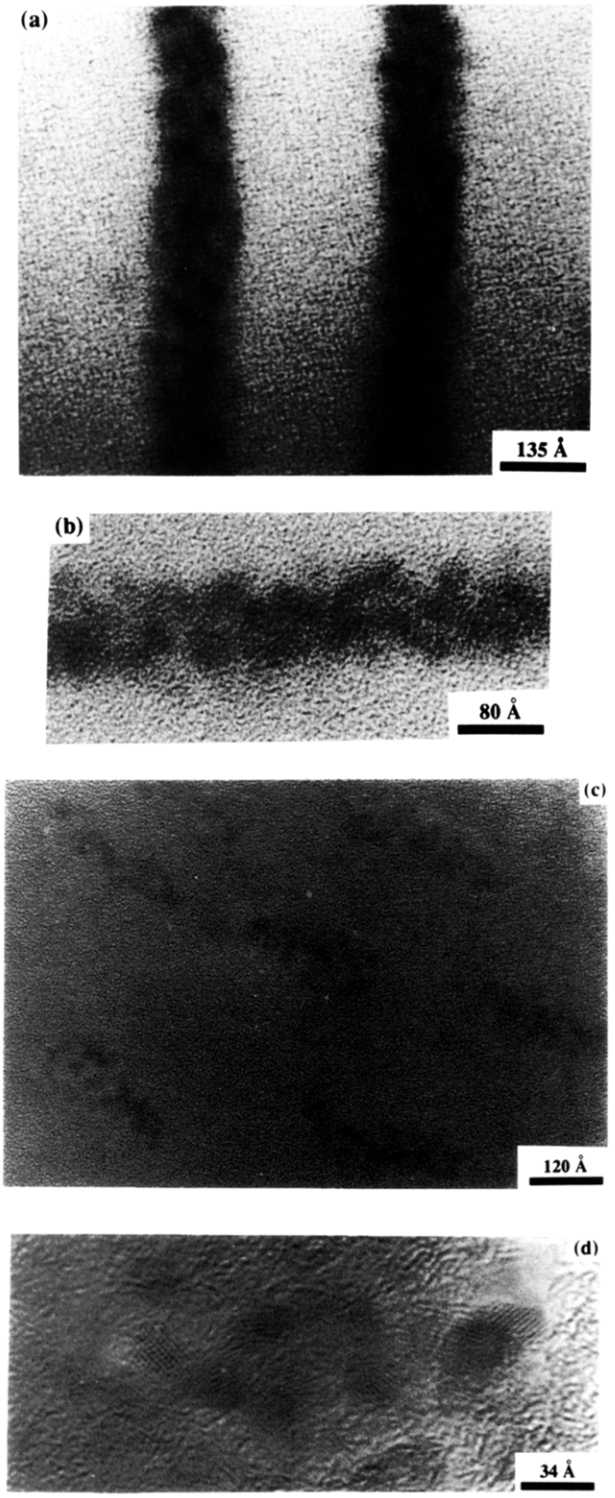

Figure 10. Representative TEM micrographs of sample A after reaction with H_2S at 180 °C: (a) bright-field image; (b) HRTEM image. Typical micrographs obtained for sample B after reaction with H_2S at high temperature: (c) bright-field image; (d) HRTEM micrograph.

same extent; yet Py enhances the cluster size and 2,6-lutidine does not. The single common feature in all of the three successful solvents is their coordinating nature; the tendency to bind with the ZnS clusters must therefore in some way be responsible for the observed increase in cluster size (see Discussion). This solvent–cluster interaction is analogous to the polymer-cluster interaction illustrated in Scheme II, with the lone pair on the nitrogen (oxygen in case of DME) forming a dative bond with the Zn atoms on the surface of the ZnS cluster. A similar effect has been observed recently by Wozniak et al. in their attempts

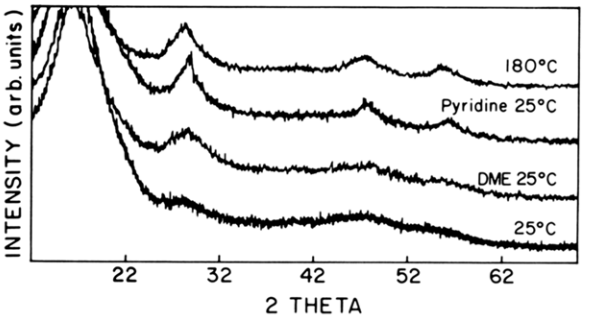

Figure 11. WAXS spectra of sample B after reaction with H_2S under various conditions.

to synthesize CdS clusters within homopolymers of vinylpyridine (PVP).[51]

XPS Characterization of ZnS Clusters. The ZnS clusters synthesized were studied by XPS to probe their electronic structure, and the results were compared to the XPS spectra of bulk ZnS (10-μm powder). Clusters synthesized at room temperature in the absence of coordinating solvents and at 180 °C were studied. To differentiate between the two types of clusters we will henceforth refer to the room temperature clusters (diameter <20 Å) as room-temperature (RT) clusters and the high-temperature (HT) clusters (diameter ~30 Å) as HT clusters. A full survey scan (0–130 eV) of the polymer films containing ZnS clusters clearly shows the presence of both Zn (2p and 3d) and S (2p) in addition to carbon and oxygen. The electronic states of the valence bands (sulfur 3p and 3s) in ZnS were not observed as their density of states is small and their coupling to the higher energy X-ray is relatively weak. Detailed scans were collected only for the sulfur 2p, the Zn 2p, and the Zn 3d peaks.

In all cases a small satellite peak on the high binding energy side was observed in the detailed scan of the S 2p peak (see Figure 12). The energy separation between the two peaks was 3.5 eV for the bulk powder, 5.7 eV for the HT clusters and 6.3 eV for the RT clusters. In the bulk sample, this satellite corresponds to the electronic transition from the valence band to the conduction band, i.e., from the S 3p to the Zn 4s band. The observed energy separation between the main and satellite peak is consistent with the bandgap energy of 3.5 eV obtained by other experimental techniques.[52,53] In the case of the clusters and particles there is no continuous band structure and the energy levels are discrete. The peak therefore corresponds to the transition from the highest occupied to the lowest unoccupied energy level, which in some sense is analogous to the bandgap. This systematic increase in band-edge separation with decreasing cluster size demonstrates the "quantum-size" effect for ZnS clusters and particles.

The detailed scans for the Zn 2p lines along with the fits obtained for the Zn 2p lines are shown in Figure 13. For the case of RT clusters (Figure 13c) the spectrum is a peak of at 1023.3 eV (fwhm of 1.9 eV) and can be fit with a single component. We attribute this component to a surfacelike species, since TEM and WAXS studies show that these particles are very small (diameter <20 Å). However, in the case of HT clusters or bulk powder, good

(51) Wozniak, M. E.; Sen, A.; Rheingold, A. L. *Chem. Mater.* **1992**, *4*, 753–755.

(52) Wheeler, R. G.; Miklosz, J. C. In *Proceedings of the International Conference on Physics of Semiconductors*; Dunod Cie: Paris, 1964; p 873.

(53) Adler, S. L. *Phys. Rev.* **1962**, *126*, 118.

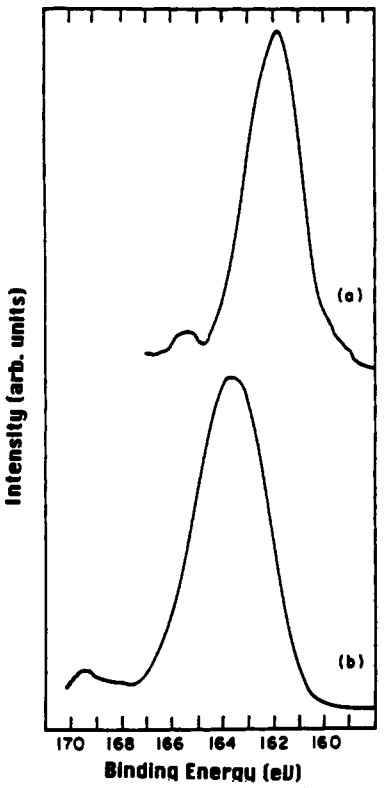

Figure 12. XPS spectra of sulfur 2p peak for (a) bulk ZnS and (b) RT clusters synthesized in sample A by reaction with H_2S at room temperature.

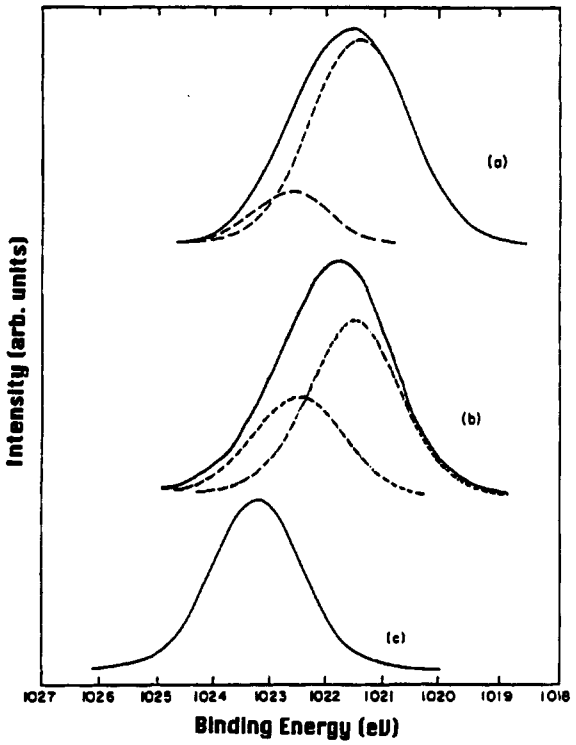

Figure 13. XPS spectra of Zn 2p core level in (a) Bulk ZnS, (b) HT clusters formed in sample A, and (c) RT clusters formed in sample A.

fits could be obtained only if there are two components in the spectrum, which we attribute to one surface core level in addition to a bulk peak. These fitting results for Zn 2p together with similar data obtained for the Zn 3d peaks are listed in Table III. In the case of bulk ZnS the surface peak is small, whereas the two peaks are of equal magnitude for the HT clusters, consistent with the larger surface-to-volume ratio of HT clusters. Also the peaks from the surface and bulk component have comparable fwhm suggesting that neither surface imperfections nor phonon broadening at the surface are important.[54]

The surface component in the clusters and the bulk powder appears at a higher mean binding energy than the bulk component by ~1.0 eV (Table III). In general, surface core-level shifts reflect changes in the potential that the electron feels in the atomic core region. There are a number of contributing factors to this change in potential: differences in screening effects, differences in electrostatic (Madelung) potential and polarization of the surrounding media for small systems.[55,56] Clearly a complete discussion of all these effects requires a full quantum mechanical treatment, which is beyond the scope of this work. It is however worthwhile to note that, on the basis of a modified Lennard-Jones and Dent equation, Watson et al.[56] estimated the binding energy of the surface orbitals in Zn to be 1.6 eV higher than the bulk orbitals. The higher surface binding energy (Table III) of the RT clusters compared to that of surface species of HT clusters and bulk powder may be caused by the polarization response to the ionization process.[55]

Discussion

Cluster Formation. The synthesis technique we have employed in this study is an in situ method where the clusters are grown within confined domains. There are two processes involved in our method: the reaction of H_2S with the organometallic polymer to form ZnS molecules followed by the aggregation of these molecules to form a cluster. Preliminary experiments with the organometallic monomer clearly indicate that the reaction step is rapid. We can therefore assume that within each domain, cluster formation essentially occurs from a homogeneous solution of ZnS molecules in the polymer, analogous to the crystallization of a solute from its supersaturated solution. Cluster formation should therefore take place via a nucleation and growth mechanism.[4,39,57]

For any spontaneous process occurring at constant temperature and pressure, the accompanying change in free energy (ΔG) must be negative. Formation of a stable nucleus therefore requires that the free energy of formation (ΔG_n, where n is the number of molecules in the nucleus) should be less than zero. ΔG_n includes contributions from two sources: the bulk energy (ΔG_v) and the surface energy (ΔG_s). ΔG_v (negative) arises from the strong attractive forces between the constituent atoms or molecules of the nucleus. It is this bulk energy which provides the driving force for nucleation and it scales as r^3 for a nucleus of radius r. ΔG_s (positive) associated with the creation of new surface, scales as r^2. ΔG_n therefore increases (becomes more positive) with r reaching a maximum value at a critical size r_c after which it decreases. All nuclei with $r < r_c$ will therefore tend to fall apart while those with $r > r_c$ will continue to grow; r_c therefore represents the minimum size for a stable nucleus. Smaller values of r_c are associated with a smaller nucleation barrier [$\Delta G_n(r=r_c)$] thereby increasing the number of stable nuclei formed. This results

(54) Van der Veen, J. F.; Heimann, P.; Himpsel, F. J.; Eastman, D. E. *Solid State Commun.* **1981**, *37*, 555.
(55) Cox, P. A. *The Electronic Structure and Chemistry of Solids*; Oxford University Press: Oxford, 1987.
(56) Watson, R. E.; Davenport, J. W.; Perlman, M. L.; Sham, T. K. *Phys. Rev. B* **1981**, *24*, 1791.
(57) Mullin, J. W. *Crystallization*; Butterworth: London, 1961.

in the formation of smaller particles when there is a limited supply of material.

Our results for the formation of zinc metal clusters in homopolymer and in lamellar block copolymers represent an excellent example of nucleation and growth behavior. The polymer matrix apparently does not interact with the zinc metal clusters and is unable to stabilize them. Therefore the Ostwald-like ripening process continues unhindered yielding extremely large (micron-sized) zinc particles. In Ostwald ripening the larger more-stable particles grow at the expense of the smaller particles. We did not, however, observe any large zinc particles in the block copolymer film exhibiting spherical morphology. This result is neither a concentration effect nor a supply problem (amount of zinc in each domain). In all films the concentration of Zn within each domain is the same and equal to the zinc atom concentration in polybTAN$(ZnPh)_2$. There is enough zinc in each domain to form a single cluster roughly 50-Å in diameter. At present we have no reasonable explanation for this curious behavior and are currently investigating it in greater detail.

Let us now consider our results for the formation of ZnS clusters. Increasing the temperature tends to destabilize the attractive forces between the molecules forming the nucleus. That is, the contribution from ΔG_v decreases at high temperatures, resulting in a larger value of r_c. The smaller nuclei will fall apart and only the large ones will continue to grow. The final particle size therefore increases as observed in our experiments. The "solvent effect" on the other hand relates to changes in the surface energy of the nuclei. The polymer tends to coordinate with the ZnS clusters via the amine group as shown in Scheme II. This interaction will tend to lower the surface energy of the cluster and stabilize it. This decrease in ΔG_s decreases r_c resulting in many stable nuclei and hence smaller clusters. Coordinating solvents such as pyridine can also bind to the cluster in competition with the polymer. A large excess of the solvent molecules could completely disrupt the polymer–cluster interaction. The surface energy of the solvent-capped clusters would of course be different from that of the polymer-capped cluster. If the solvent does a poor job of stabilizing the cluster in comparison to the polymer then ΔG_s will increase resulting in a larger r_c and hence larger clusters.

Comparison of our results for ZnS and Zn highlights the importance of the polymer–cluster interaction. Without the stabilizing effect of such an interaction it was not possible to make domain-controlled Zn clusters even in a glassy matrix; the interaction is essential for the long-term stability of the clusters. The strong ZnS polymer interaction does make it more difficult to make large clusters, but as we have already shown this can be overcome. The polymer–cluster interaction can be altered by using suitable solvents during the cluster-synthesis process. Alternatively, one could manipulate the structure of the polymer so as to weaken the interaction and allow for the formation of larger clusters.

Cluster Characterization. As is obvious from our TEM micrographs there are multiple clusters formed within each domain and these are randomly distributed. The clusters synthesized ranged in size up to about 30 Å depending on the synthesis conditions, the largest clusters being formed by the high-temperature synthesis method. We did not do any quantitative analysis of the TEM data, but it is obvious that there is substantial variation in the size of clusters formed; however the ZnS clusters are always restricted within the domains. Therefore on the global scale there is an organized and well-defined distribution of clusters in the polymer matrix. The implications of this with respect to the properties of these polymer–cluster composites is as yet unclear. Our efforts at investigating the electronic structure of these composites by optical spectroscopy have been hindered by the nature of the MTD matrix. The double bonds in polyMTD react with H_2S to form some product which strongly absorbs in the same wavelength range as the clusters. We are currently in the process of determining ways of hydrogenating the MTD block prior to H_2S treatment to overcome this problem.

The XPS approach provides an alternative method of obtaining some information on the optical properties of these composite materials. The bandgap for the cluster is easily obtained from the position of the shakeup peak. As expected the bandgap increases with decreasing cluster size. The observed 2.8-eV increase in the bandgap from bulk material to the RT clusters compares well with the theoretical calculations of Lippens and Lannoo.[58] On the basis of the tight-binding approximation and recursion methods they calculated the size dependence of the bandgap for small spherical ZnS clusters over a wide range of cluster size. Their calculations for a cluster containing 17 atoms with diameter of 8.6 Å predict a 2.5-eV increase in the band-edge separation relative to the bulk value, in good agreement with our observations.

Conclusion

The technique of synthesizing semiconductor clusters within microphase-separated block copolymer films successfully allows for the formation of domain controlled ZnS clusters. Multiple clusters are formed within each domain with typical cluster sizes ranging up to 30 Å in diameter. The size primarily depends on two parameters: synthesis temperature and the strength of the polymer–cluster interaction. The effect of these parameters can be well understood within the framework of the nucleation theory. It is the polymer–cluster interaction which stabilizes the small clusters and inhibits any kind of Ostwald-like ripening process from taking place. Cluster size is therefore very closely related to the strength of the interaction between the polymer and the cluster. This interaction can be modified by the use of suitable coordinating solvents in the cluster synthesis process.

As expected, the ZnS clusters exhibit quantum-size effects, with the band-edge separation increasing with a decrease in cluster size. A roughly spherical ZnS cluster of ~30-Å diameter has a bandgap of 5.7 eV. Further characterization of the optical properties of these clusters is in progress. Additionally we are developing other copolymer systems in which the polymer–cluster interaction is weaker than in the MTD/bTAN system and this should facilitate synthesis of clusters larger than 30 Å.

Acknowledgment. This research was supported primarily by NSF, Division of Chemistry, under Grant CHE 9007175. We thank M. Frongillo of the C.M.S.E.-Electron Microscopy Facility at M.I.T. for invaluable technical assistance in HRTEM studies.

(58) Lippens, P. E.; Lannoo, M. *Phys. Rev. B* **1989**, *39*, 10935.